Supporting Information

Newly developed palladium complexes featuring ONS donor ligands: Synthetic method, characterization, CT-DNA, BSA protein binding study and in-vitro cytotoxicity

Arpan Halder [a], Akash Das [a], Subhabrata Guha [b], Gaurav Das [b], Rahul Naskar [a] and Tapan K. Mondal [*a]

[a]Department of Chemistry, Jadavpur University, Kolkata- 700032, India. E-mail: tapank.mondal@jadavpuruniversity.in

[b]Department of Signal Transduction and Biogenic Amines (STBA), Chittaranjan National Cancer Institute, Kolkata- 700026, India.

CONTENTS

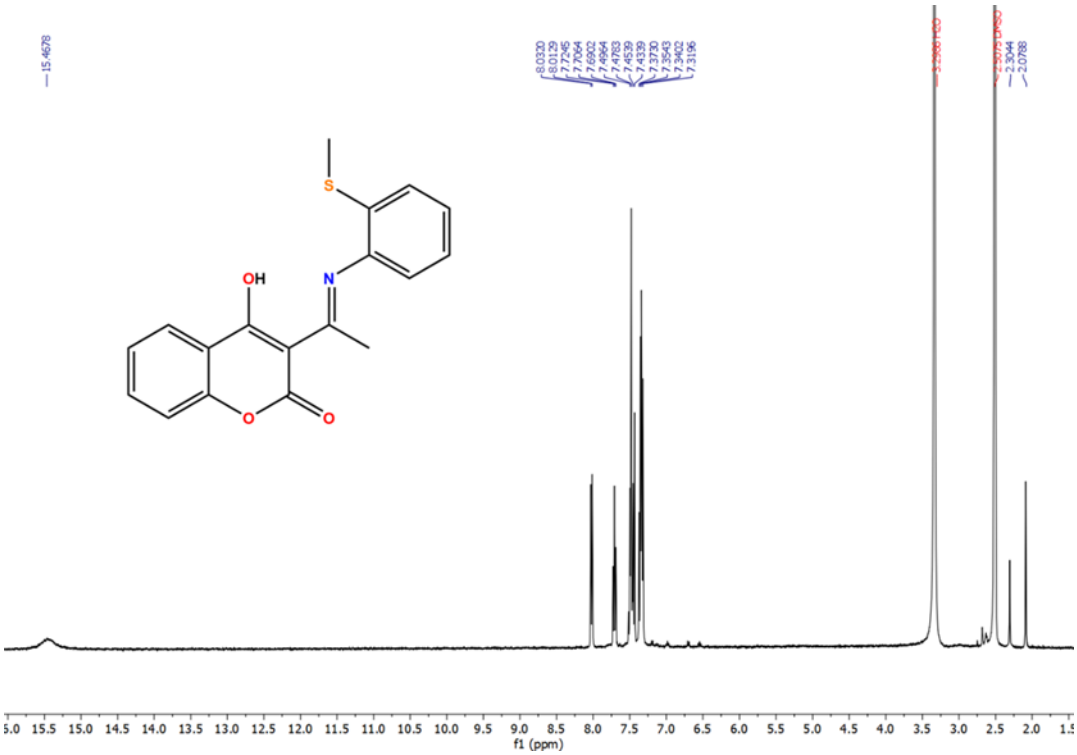

Fig. S1: ^{1}H NMR spectrum of **HL^{1}** in DMSO-D_6

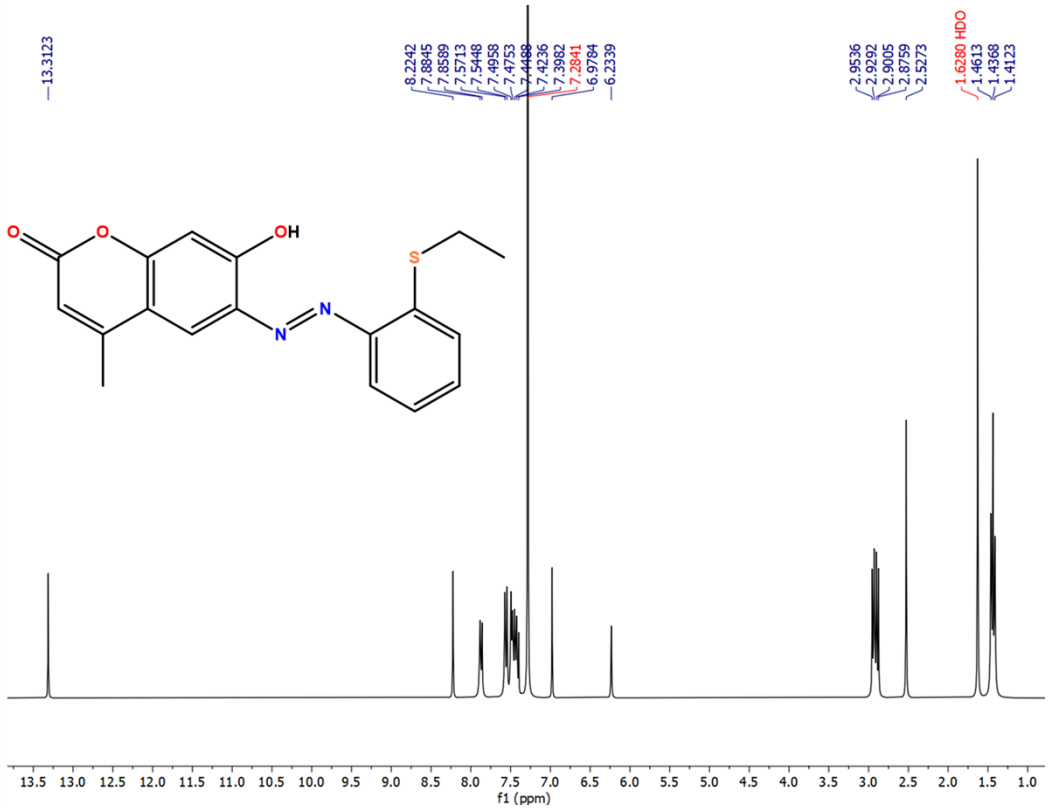

Fig. S2: ^{1}H NMR spectrum of **HL^{2}** in $CDCl_3$

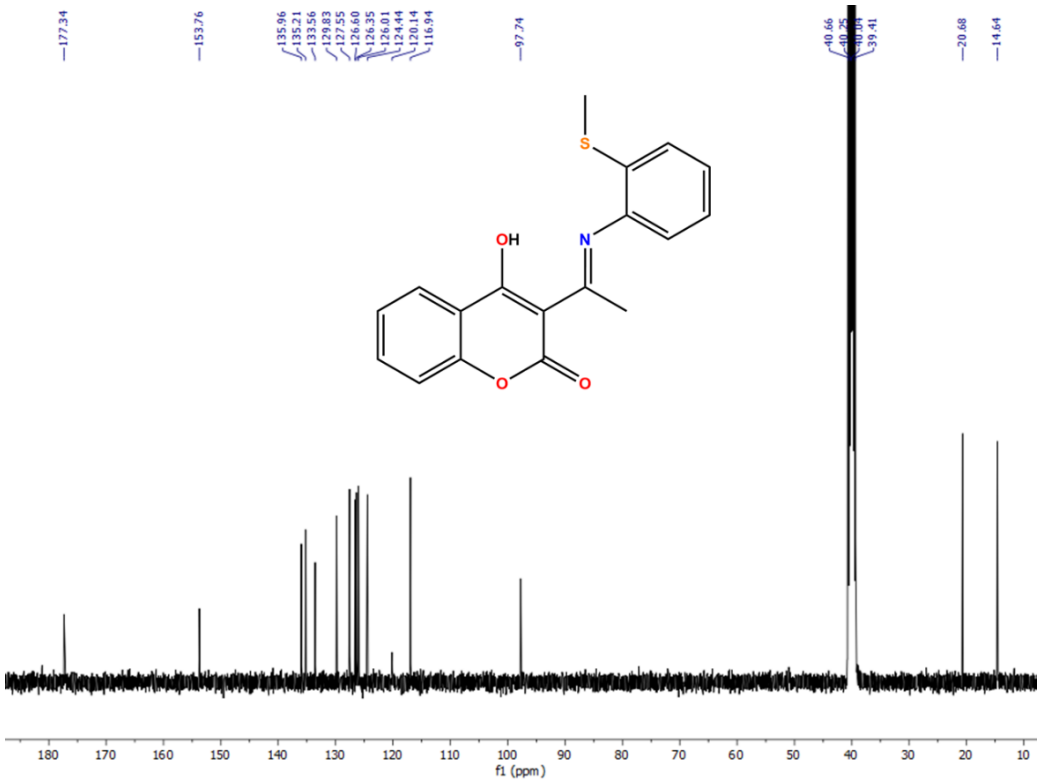

Fig. S3: ^{13}C NMR spectrum of ligand **HL^1** in DMSO-D_6

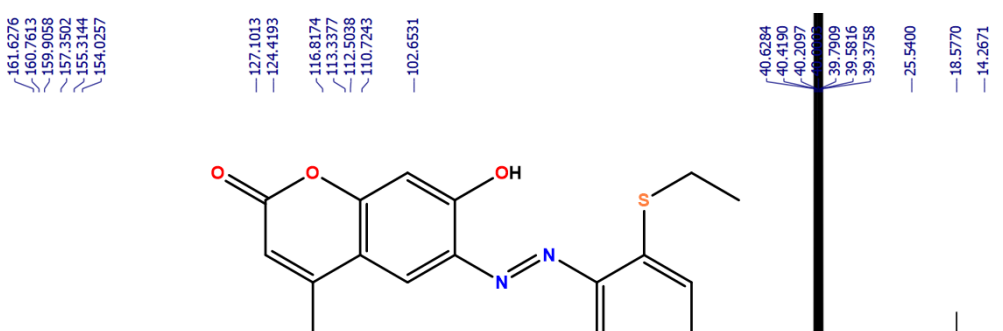

Fig. S4: ^{13}C NMR spectrum of ligand **HL²** in $CDCl_3$

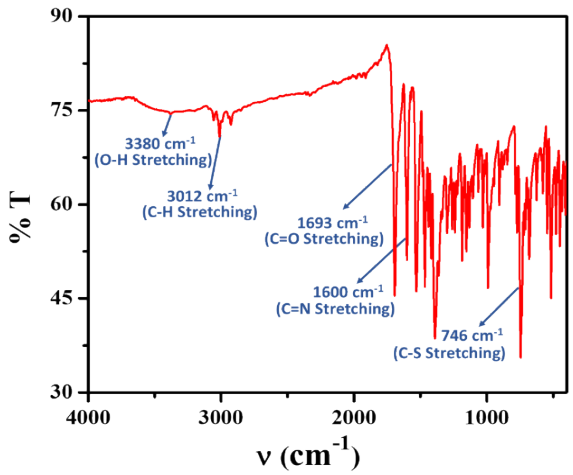

Fig. S5: IR spectrum of ligand **HL**[1]

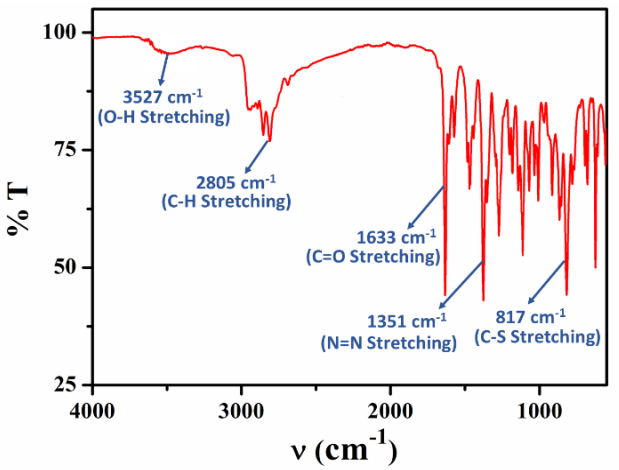

Fig. S6: IR spectrum of ligand **HL**[2]

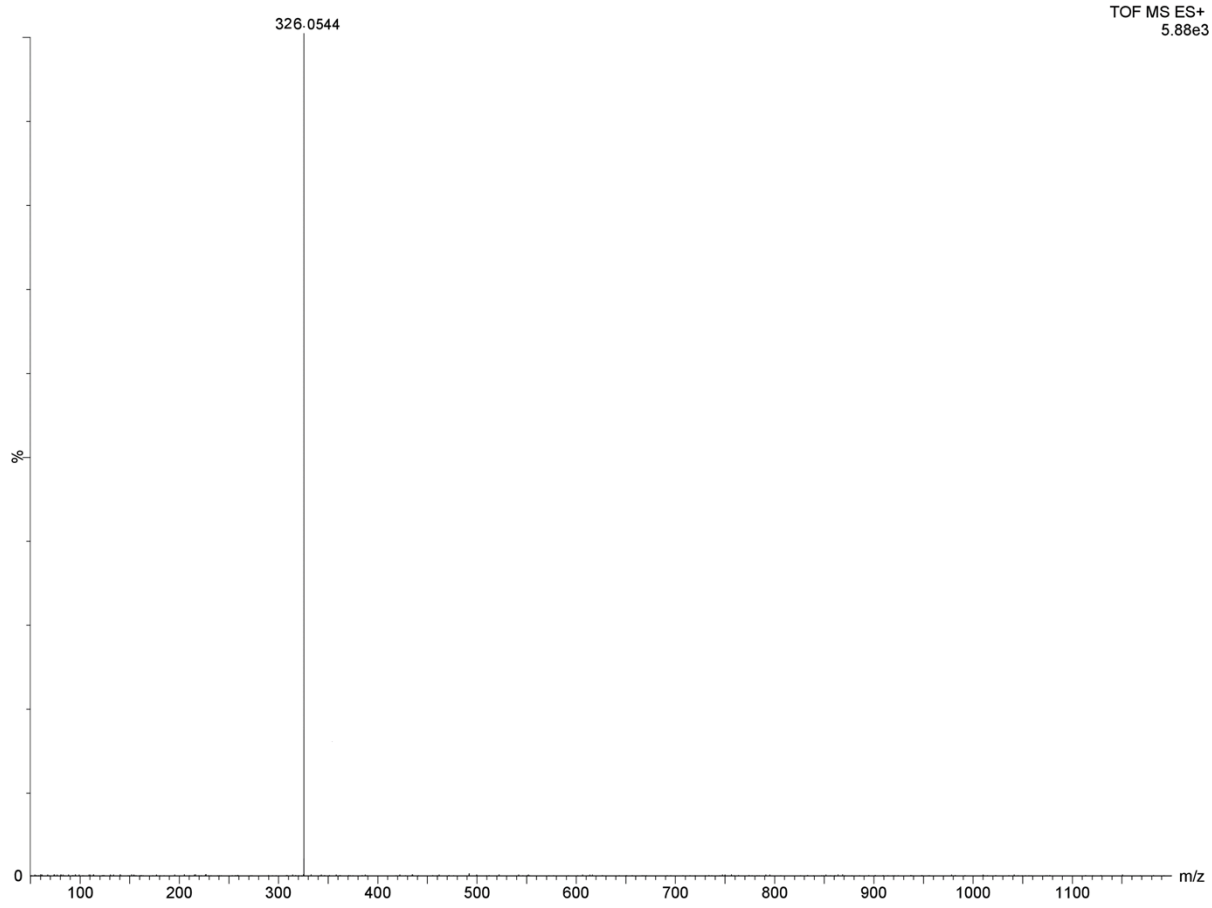

Fig. S7: HRMS of ligand **HL**[1] in methanol

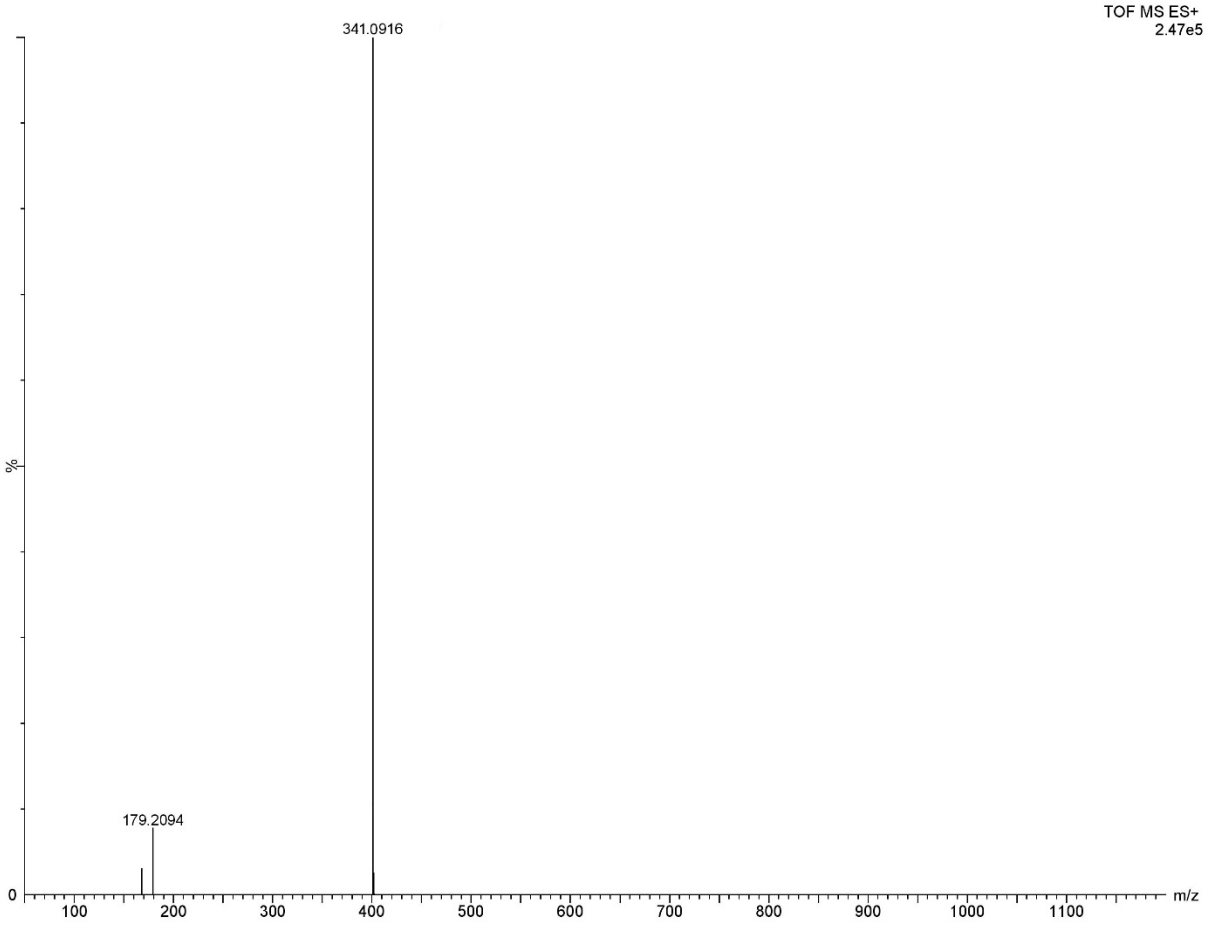

Fig. S8: HRMS of ligand **HL²** in methanol

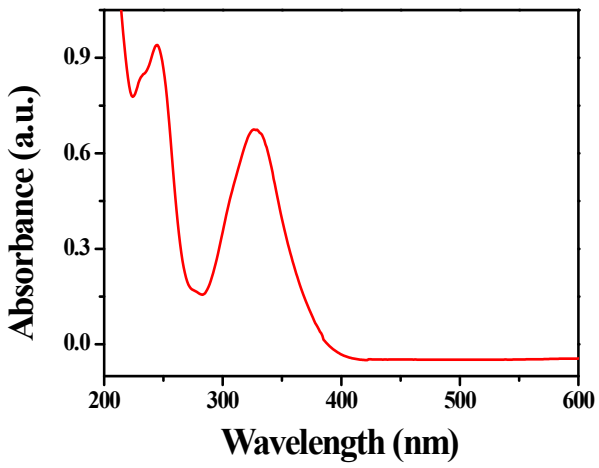

Fig. S9: Absorption spectra of ligand **HL¹** in acetonitrile

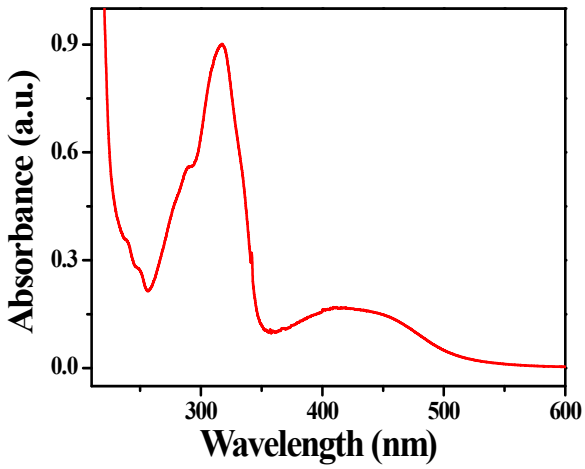

Fig. S10: Absorption spectra of ligand **HL²** in acetonitrile

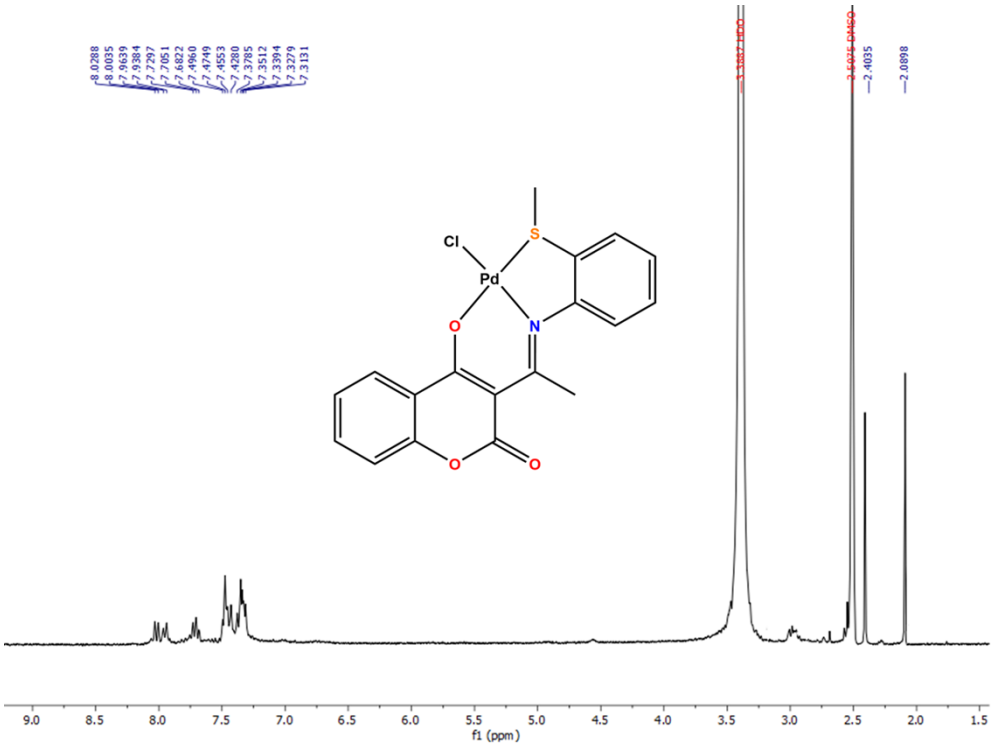

Fig. S11: ^{1}H NMR spectrum of **C1** in DMSO-D_6

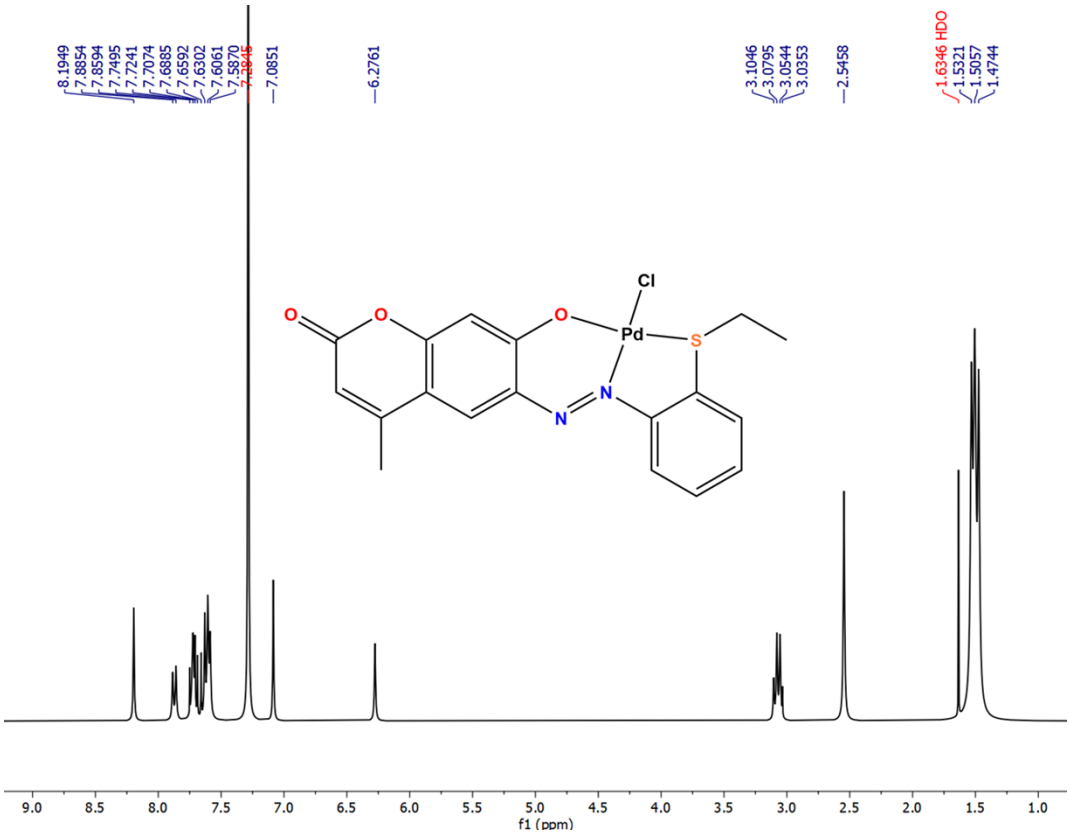

Fig. S12: ^{1}H NMR spectrum of **C2** in $CDCl_3$

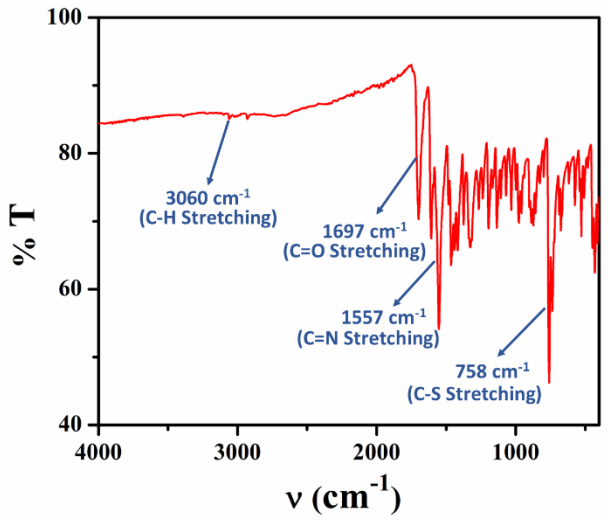

Fig. S13: IR spectrum of ligand **C1**

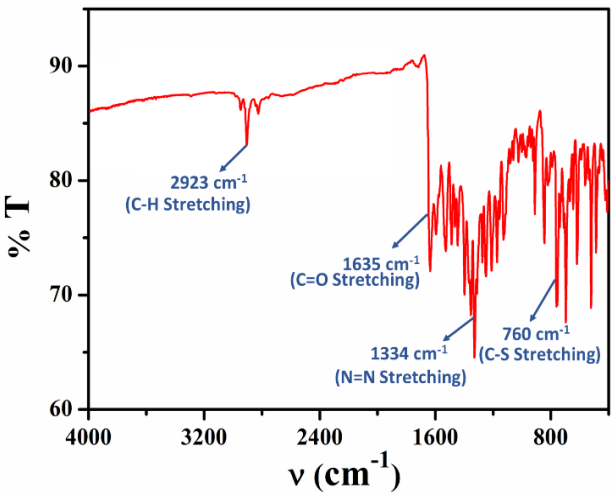

Fig. S14: IR spectrum of ligand **C2**

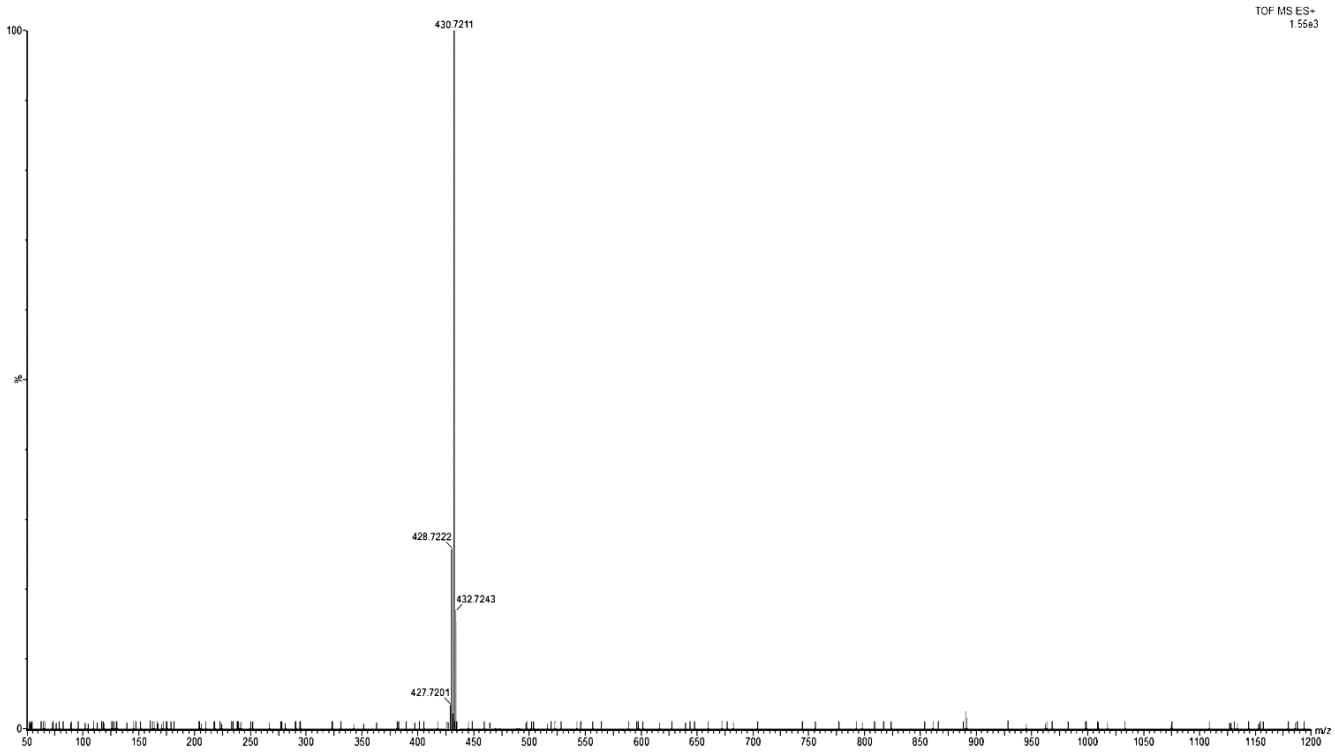

Fig. S15: HRMS of **C1** in methanol

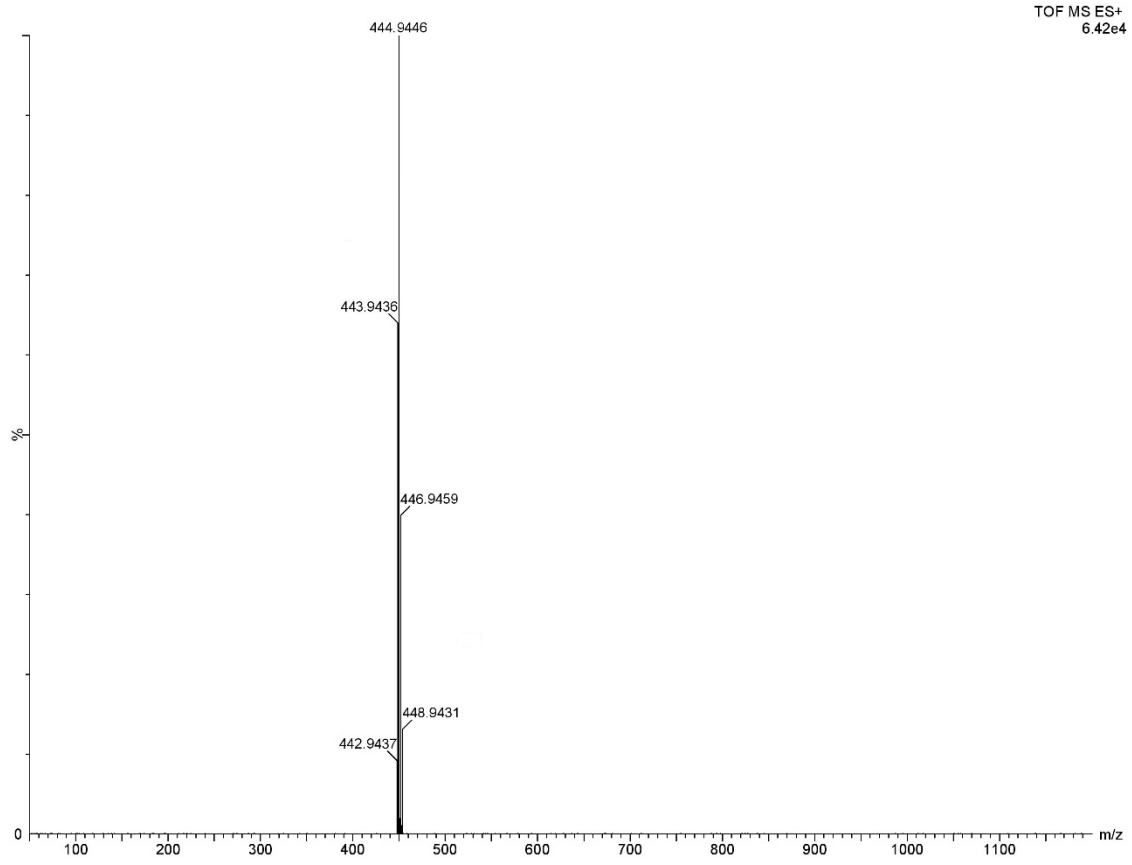

Fig. S16: HRMS of ligand **C2** in methanol

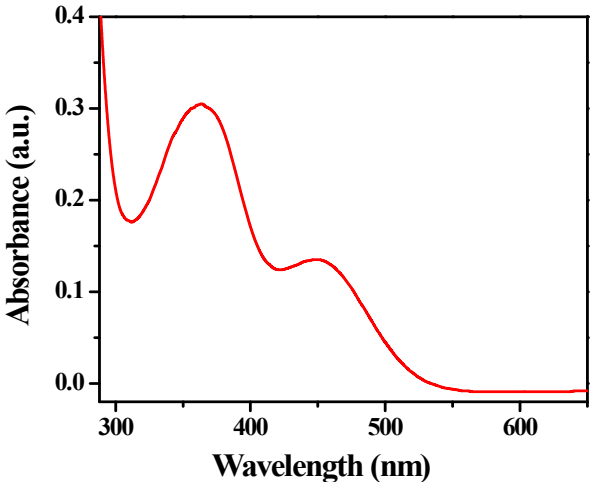

Fig. S17: Absorption spectra of **C1** in DMSO

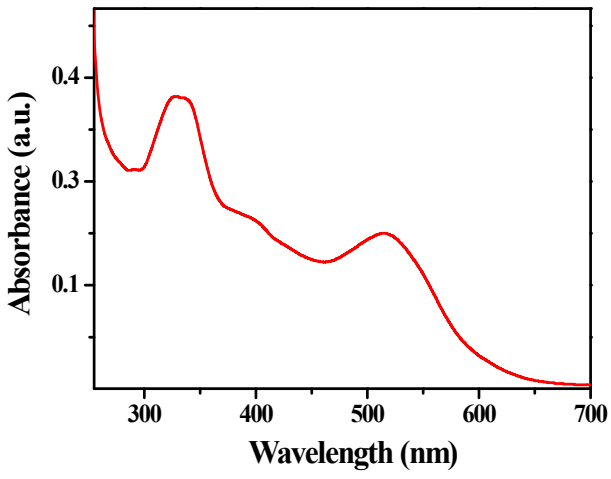

Fig. S18: Absorption spectra of **C2** in DMSO

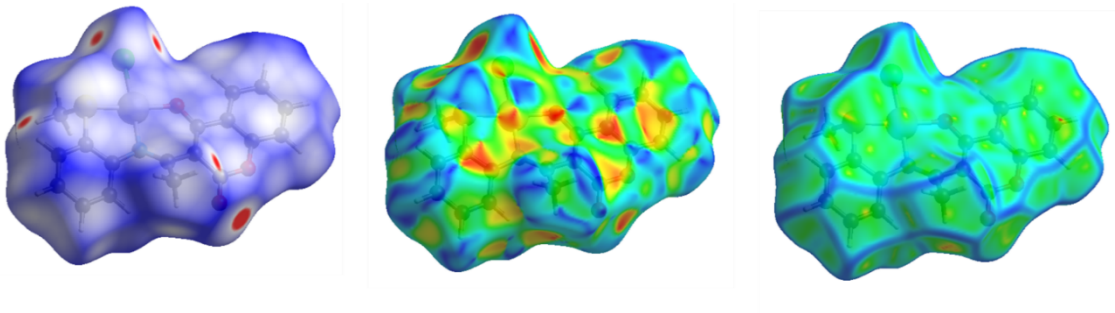

Fig. S19: Hirshfeld surfaces of **C1** mapped with d_{norm} (left-side), shape index (middle) and curvedness (right-side)

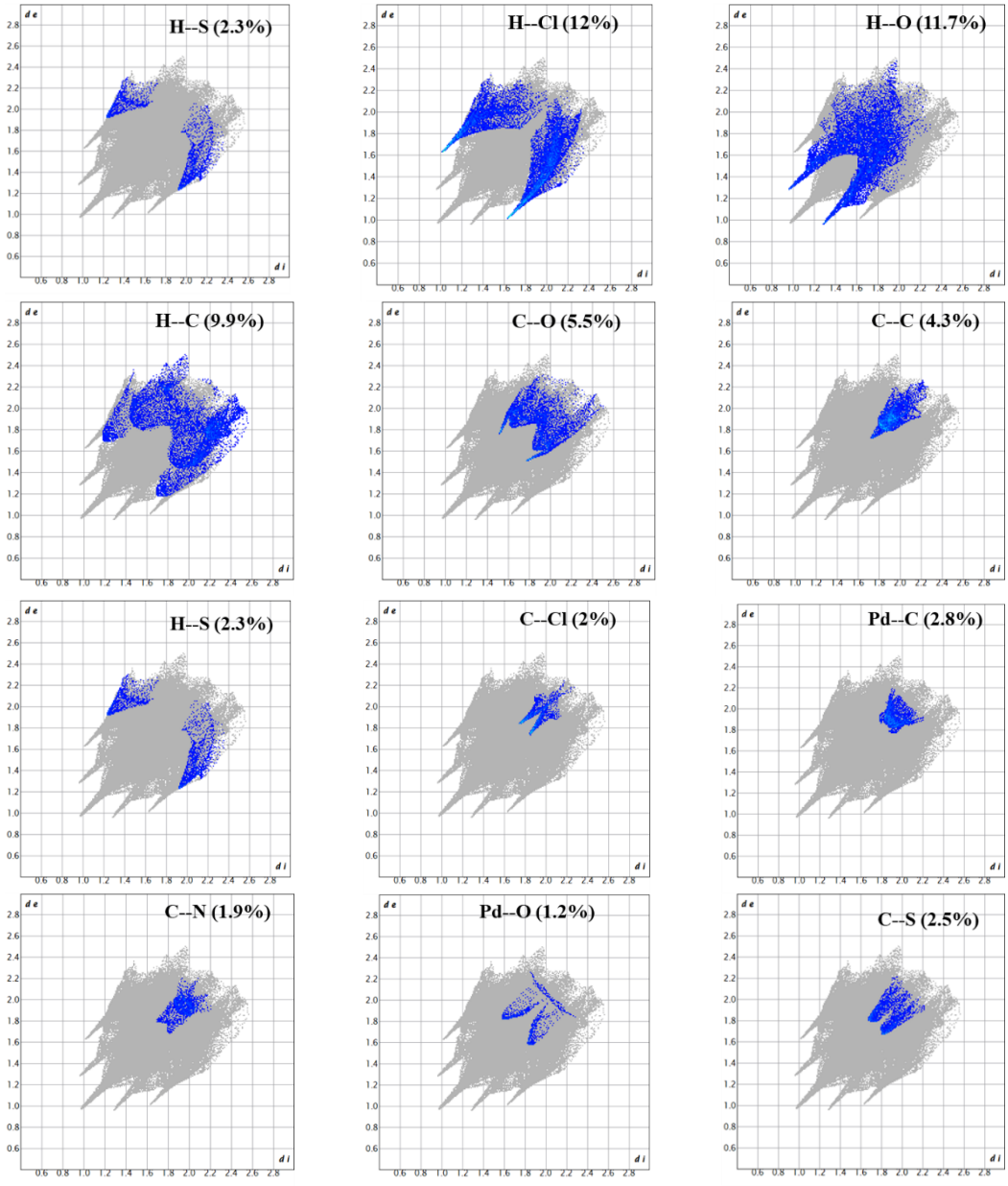

Fig. S20: 2D Fingerprint plot resolved into different contacts contributed to the total Hirshfeld Surface area of the **C1**

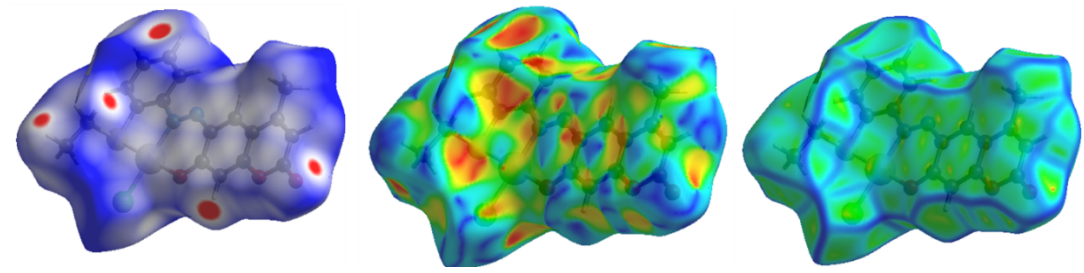

Fig. S21: Hirshfeld surfaces of **C2** mapped with d_{norm} (left-side), shape index (middle) and curvedness (right-side)

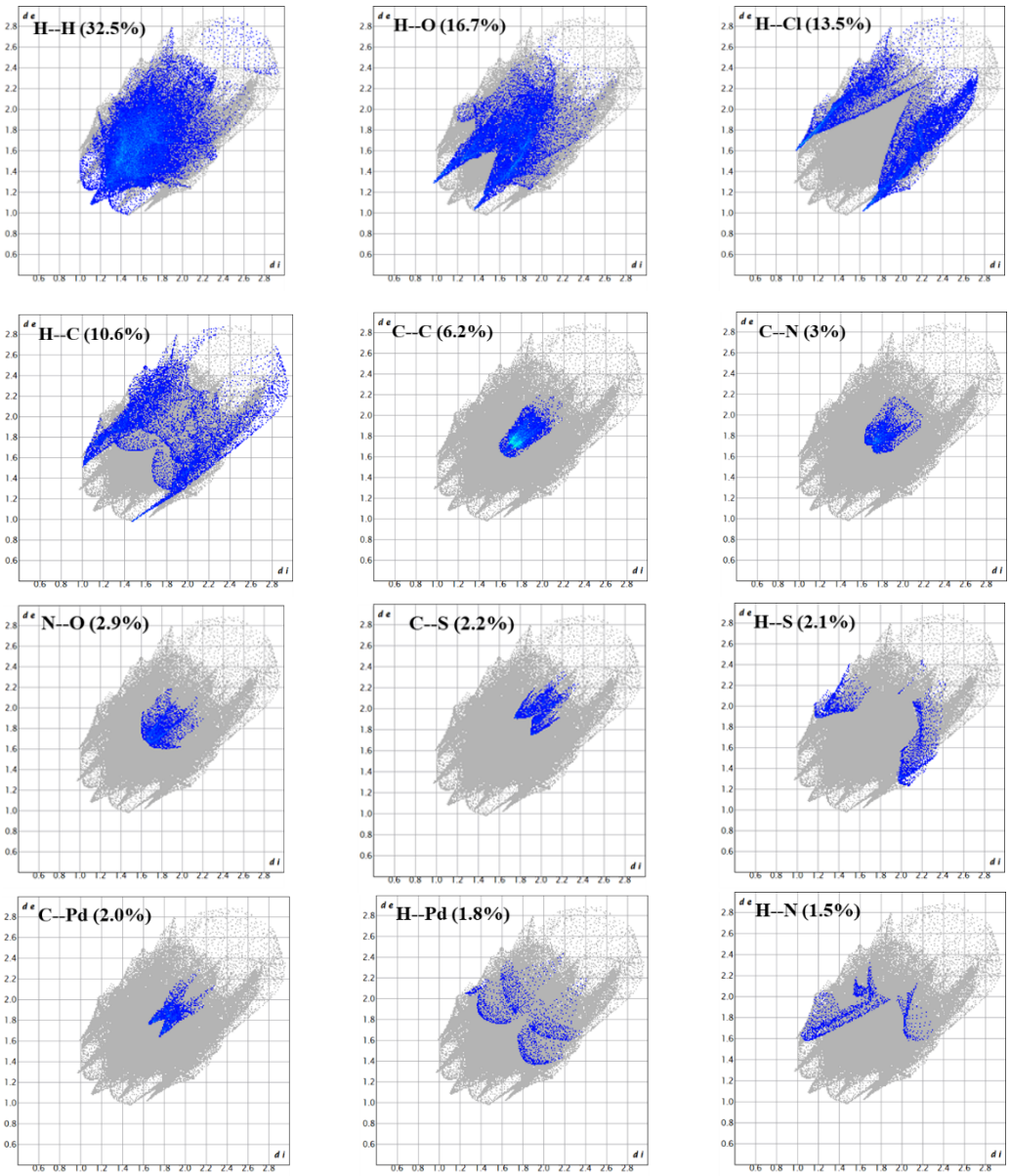

Fig. S22: 2D Fingerprint plot resolved into different contacts contributed to the total Hirshfeld Surface area of the **C2**

Table S1: Crystallographic data and refinement parameters of **C1** and **C2**

	C1	**C2**
Empirical formula	$C_{18}H_{14}NO_3ClPdS$	$C_{18}H_{15}ClN_2O_3PdS$
Formula weight	466.21	481.23
Temperature/K	293	293(2)
Crystal system	monoclinic	triclinic
Space group	*C2/c*	$P\bar{1}$
a, b, c (Å)	25.223(2), 10.8041(9), 14.5920(12)	8.5320(8), 15.0214(14), 15.0214(14)
α, β, γ (°)	90, 122.365(2), 90	83.277(2), 76.249(2), 76.249(2)
Volume/Å^3	3358.8(5)	1812.7(3)
Z	8	4
ρ_{calc}g/cm^3	1.844	1.763
μ/mm^{-1}	1.406	1.307
F(000)	1856	960
Radiation	MoKα (λ = 0.71073)	MoKα (λ = 0.71073)
θ(Min-Max) (°)	2.982–27.509	2.518–26.153
Index ranges	-32 ≤ h ≤ 32, -14 ≤ k ≤ 14, -18 ≤ l ≤ 18	-10 ≤ h ≤ 10, -18 ≤ k ≤ 18, -18 ≤ l ≤ 18
Reflections collected	51896	24400
Independent reflections	3844 (R_{int} = 0.0639, R_{sigma} = 0.0232)	7193 (R_{int} = 0.0396, R_{sigma} = 0.0446)
Data/restraints/parameters	3844/0/229	7193/0/473
Final R indexes [I>=2σ (I)]	R_1 = 0.0343, wR_2 = 0.0750	R_1 = 0.0403, wR_2 = 0.0794
Final R indexes [all data]	R_1 = 0.0372, wR_2 = 0.0766	R_1 = 0.0634, wR_2 = 0.0902
Largest diff. peak/hole / e Å^{-3}	0.63/-0.59	0.50/-0.42
ccdc no.	2359962	2359963

Table S2: Selected X-ray and calculated bond distances and angles of **C1**

Bond Lengths (Å)	X-ray	Calc.
Pd1–S1	2.2174(9)	2.304
Pd1–Cl1	2.3036(8)	2.335
Pd1–N1	2.019(3)	2.039
Pd1–O1	1.982(2)	2.008
S1–C17	1.776(3)	1.815
S1–C18	1.810(4)	1.838
N1–C10	1.325(4)	1.337
N1–C12	1.433(4)	1.419
O1–C1	1.276(4)	1.274
O2–C7	1.361(5)	1.359
O2–C8	1.381(5)	1.391
O3–C8	1.197(5)	1.213
Bond Angles (°)		
S1–Pd1–Cl1	88.29(3)	91.513
N1–Pd1–S1	88.38(8)	86.766
N1–Pd1–Cl1	176.64(8)	178.119
O1–Pd1–S1	175.03(8)	176.904
O1–Pd1–Cl1	89.28(7)	91.403
O1–Pd1–N1	94.02(10)	90.304
C17–S1–Pd1	98.20(11)	95.665
C18–S1–Pd1	104.69(16)	105.123
C10–N1–Pd1	121.9(2)	122.105
C12–N1–Pd1	114.8(2)	114.014
C1–O1–Pd1	124.6(2)	125.353

Table S3: Selected X-ray and calculated bond distances and angles of **C2**

Bond Lengths (Å)	**C1**	
	X-ray	Calc.
Pd1–S1	2.2404(11)	2.300
Pd1–Cl1	2.3118(12)	2.3389
Pd1–N1	1.983(3)	2.019
Pd1–O1	1.992(3)	2.019
Pd2–S2	2.2493(11)	-
Pd2–Cl2	2.3065(13)	-
Pd2–N3	1.984(3)	-
Pd2–O4	1.998(3)	-
S1–C1	1.783(4)	1.797
S1–C17	1.806(5)	1.857
S2–C19	1.778(5)	-
S2–C35	1.843(5)	-
O1–C16	1.291(5)	1.284
O4–C34	1.288(5)	-
N1–N2	1.269(4)	1.276
N3–N4	1.275(4)	-
Bond Angles (°)		
S1–Pd1–Cl1	90.16(4)	89.928
O1–Pd1–Cl1	89.68(9)	91.129
O1–Pd1–S1	179.68(9)	177.944
N1–Pd1–Cl1	177.35(10)	176.169
N1–Pd1–S1	87.57(10)	86.988
N1–Pd1–O1	92.59(12)	92.023
S2–Pd2–Cl2	91.48(4)	-
O4–Pd2–Cl2	88.78(9)	-
O4–Pd2–S2	178.42(9)	-
N3–Pd2–Cl2	178.71(10)	-
N3–Pd2–S2	87.29(10)	-
N3–Pd2–O4	92.44(12)	-

Table S4: Energy and % of composition of some selected molecular orbitals of **C1**

MO	Energy (eV)	% Composition		
		Pd	L^1	Cl
LUMO+5	-0.12	50	50	00
LUMO+4	-0.37	09	91	00
LUMO+3	-1.06	03	97	00
LUMO+2	-1.32	04	96	00
LUMO+1	-2.02	17	78	05
LUMO	-2.66	22	7	08
HOMO	-6.06	17	64	19
HOMO-1	-6.55	16	10	77
HOMO-2	-6.62	09	65	26
HOMO-3	-6.72	09	56	35
HOMO-4	-6.87	71	25	04
HOMO-5	-7.12	26	71	03
HOMO-6	-7.32	03	85	12
HOMO-7	-7.44	07	88	05
HOMO-8	-7.63	04	93	07
HOMO-9	-7.89	46	45	09
HOMO-10	-8.21	50	29	21

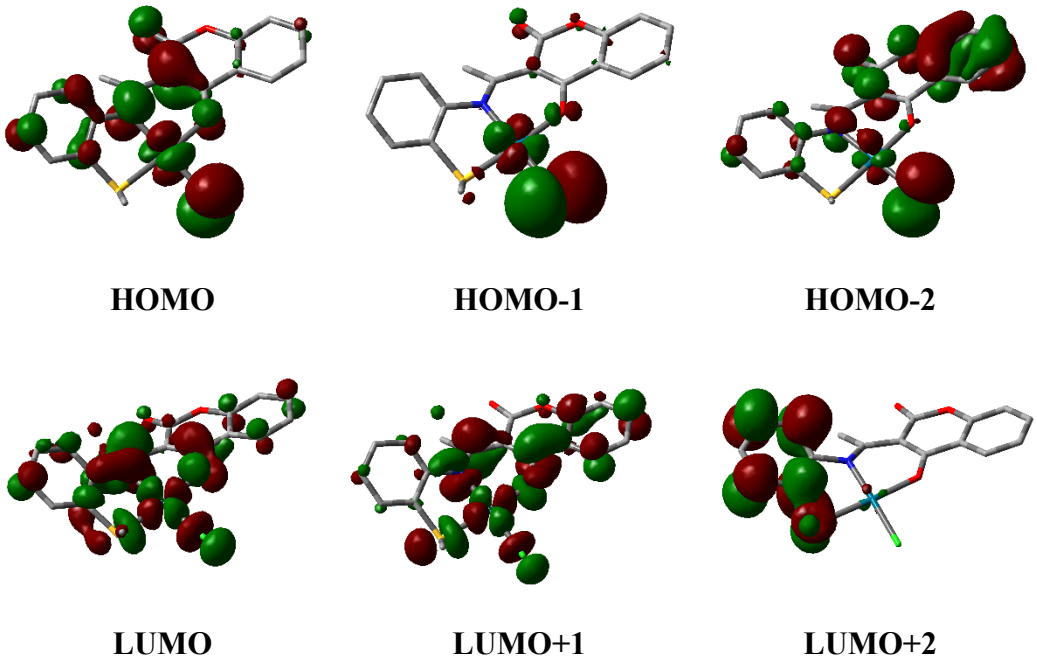

Fig. S23: Contour plots of some selected molecular orbital of **C1**

Table S5: Vertical electronic transitions calculated by TDDFT/CPCM method of **C1**

λ (nm)	E (eV)	Osc. Strength (f)	Key excitations	Character	$\lambda_{expt.}$ (nm) (ε, $M^{-1}cm^{-1}$)
517.9	2.3940	0.0386	(77%)HOMO→LUMO	MLCT/XLCT/ILCT	450 (10856)
468.5	2.6464	0.0129	(55%)HOMO-1→LUMO (31%)HOMO-2→LUMO	XLCT/ILCT MLCT/XLCT	
393.1	3.1536	0.1414	(69%)HOMO-1→LUMO+1	XLCT/ILCT	
364.9	3.3980	0.1472	(76%)HOMO-3→LUMO+1	ILCT/XLCT	363 (24488)
307.9	4.0262	0.1135	(80%)HOMO-6→LUMO	ILCT	

Table S6: Energy and % of composition of some selected molecular orbitals of **C2**

MO	Energy (eV)	% Composition		
		Pd	L^2	Cl
LUMO+5	-0.1	84	16	00
LUMO+4	-0.67	01	99	00
LUMO+3	-1.51	03	97	00
LUMO+2	-1.68	00	100	00
LUMO+1	-2.32	47	39	14
LUMO	-3.1	03	97	00
HOMO	-5.96	18	71	11
HOMO-1	-6.55	17	36	47
HOMO-2	-6.59	15	08	77
HOMO-3	-6.82	05	77	18
HOMO-4	-7.05	74	14	12
HOMO-5	-7.36	13	65	21
HOMO-6	-7.49	20	76	04
HOMO-7	-7.58	00	98	02
HOMO-8	-7.67	09	87	03
HOMO-9	-8.07	41	59	00
HOMO-10	-8.32	44	42	13

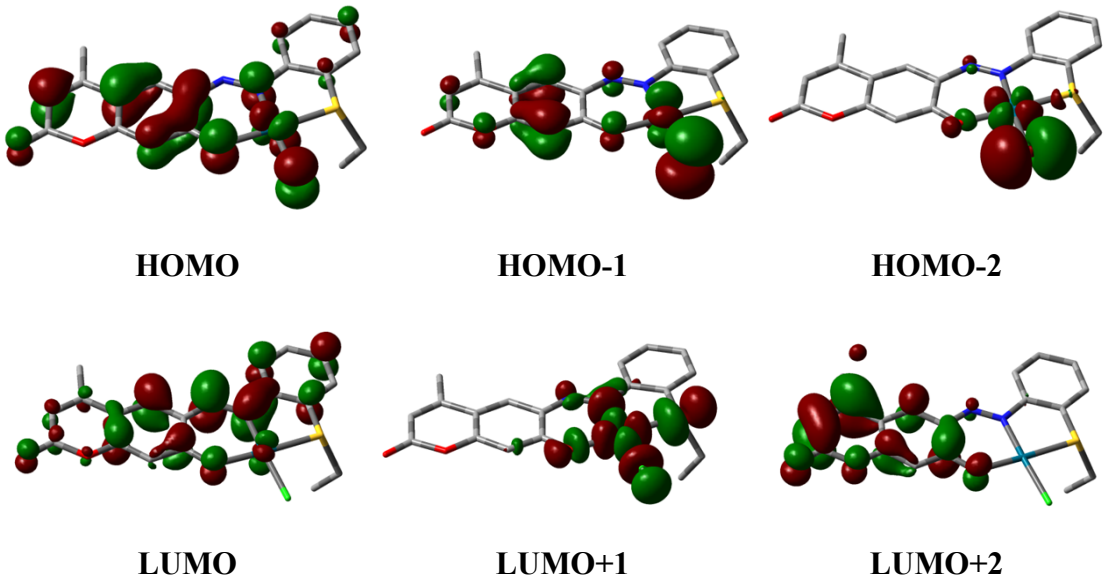

Fig. S24: Contour plots of some selected molecular orbital of **C2**

Table S7: Vertical electronic transitions calculated by TDDFT/CPCM method of **C2**

λ (nm)	**E (eV)**	**Osc. Strength (f)**	**Key excitations**	**Character**	**$\lambda_{expt.}$ (nm) (ε, $M^{-1}cm^{-1}$)**
502.4	2.4677	0.2440	(88%)HOMO→LUMO	MLCT/ILCT	515 (16099)
478.5	2.5909	0.0131	(89%)HOMO-1→LUMO	MLCT/ILCT/XLCT	
376.9	3.2898	0.2210	(70%)HOMO-3→LUMO	ILCT/XLCT	396 (sh.)
358.1	3.4623	0.1528	(68%)HOMO-3→LUMO	ILCT	
325.9	3.8041	0.1961	(52%)HOMO→LUMO+2	ILCT	330 (29964)
312.4	3.9686	0.2418	(37%)HOMO-6→LUMO	ILCT	

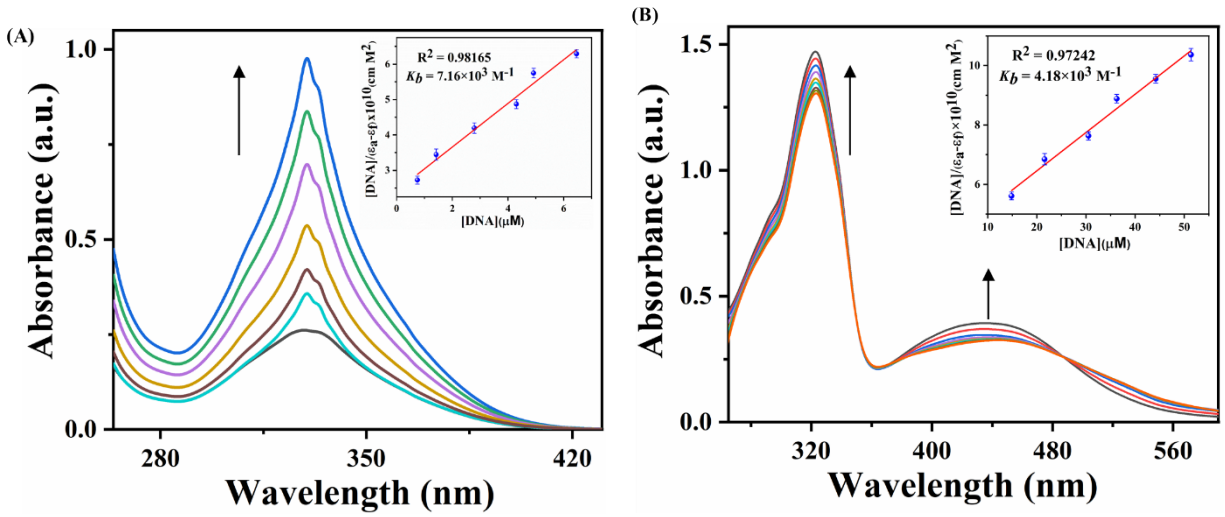

Fig. S25: Change in absorption spectra of the **HL¹** (A) and **HL²** (B) with the gradual addition of CT DNA. Inset: Plot of [DNA]/($\varepsilon_a - \varepsilon_f$) vs. [DNA].

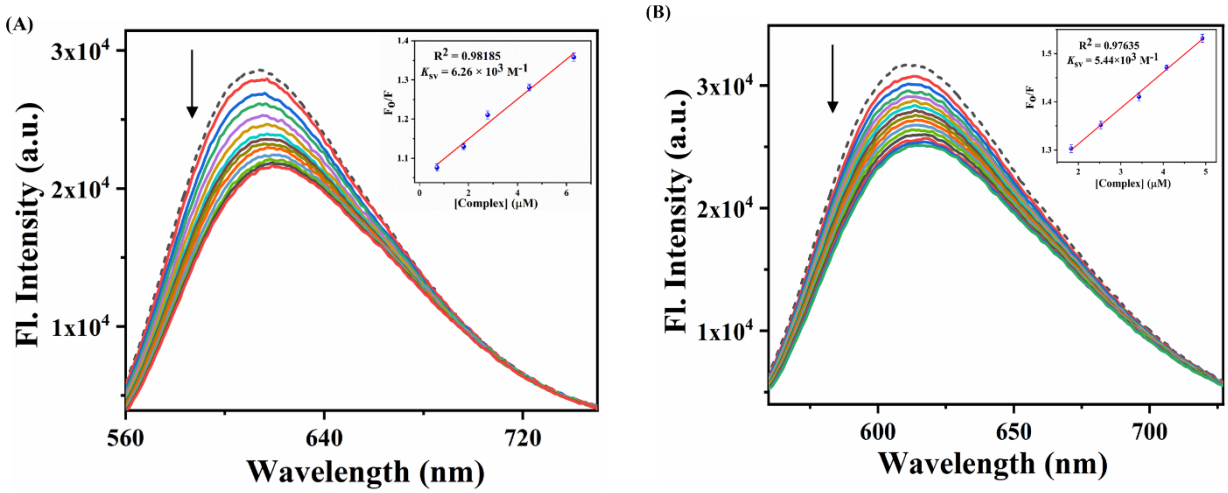

Fig. S26: Emission spectra of EB-CT DNA with increasing concentrations of the **HL¹** (A) and **HL²** (B). Inset: Plots of emission intensity F0/F vs. [Complex].

Table S8: Comparison table of K_{SV} of similar palladium complexes.

Complex	*Ksv* (M^{-1})	Ref
C1	2.45×10^5	This work
C2	1.51×10^5	
Pd1	9.71×10^5	50
Pd2	23.14×10^5	
Pd3	28.41×10^5	
Pd4	1.82×10^5	
$[Pd(PPh_3)L]$	4.75×10^4	51
$[Pd(AsPh_3)L]$	3.03×10^4	
$[Pd(L)_2]$	5.87×10^4	52
$[\{Pd(en)Cl\}_2(\mu\text{-}4,4'\text{-bipy})](NO_3)_2$	7.8×10^4	53
$[\{Pd(en)Cl\}_2(\mu\text{-bpa})](NO_3)_2$	1.7×10^4	
$[\{Pd(en)Cl\}_2(\mu\text{-bpe})](NO_3)_2$	9.9×10^4	
C1	2.64×10^4	54
C2	9.61×10^3	
C3	1.20×10^4	
C4	1.02×10^5	
PdL1	5.30×10^5	55
PdL1	2.46×10^5	

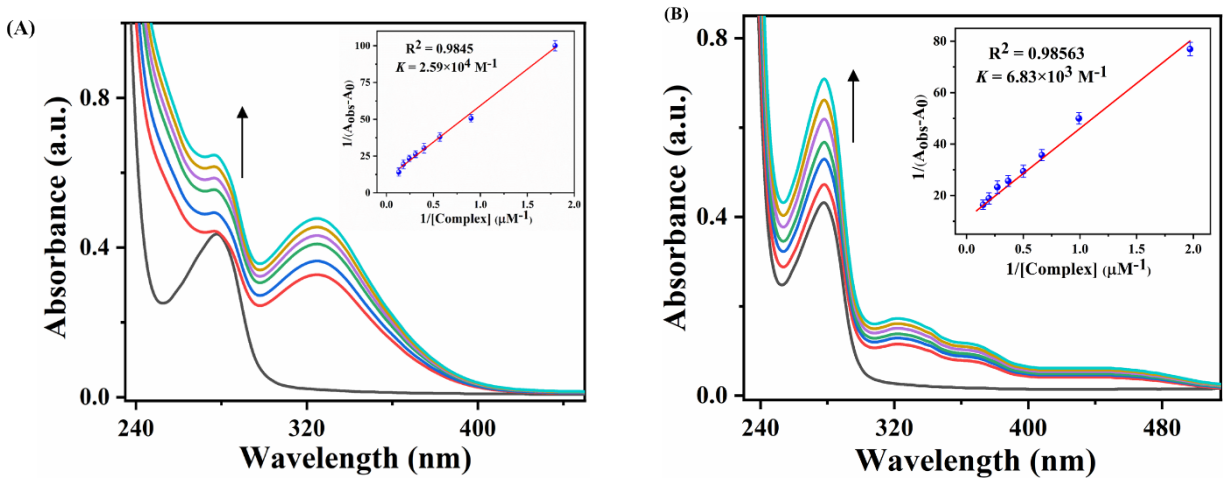

Fig. S27: Change in absorption spectra of BSA with the increasing addition of **HL¹** (A) and **HL²** (B). Inset: Plot of $1/(A_{obs}\text{-}A_0)$ vs 1/[Complex].

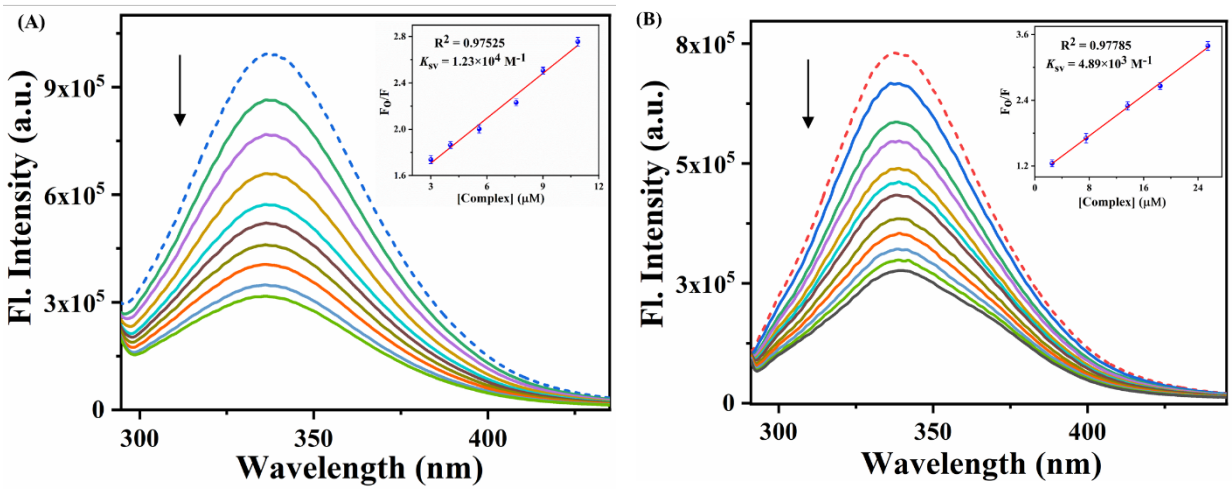

Fig. S28: Emission spectra of BSA in presence of gradual increase in concentrations of **HL^1** (A) and **HL^2** (B). Inset: Plots of emission intensity F0/F vs. [Complex].

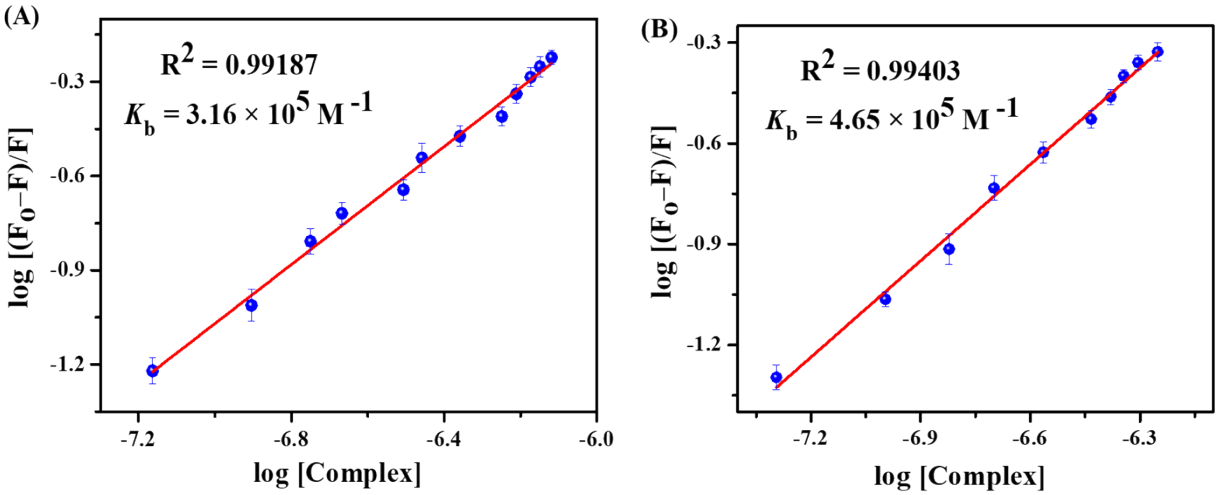

Fig. S29: Plot of log [(Fo-F)/F] versus log [Complex] for **C1** (A) and **C2** (B).

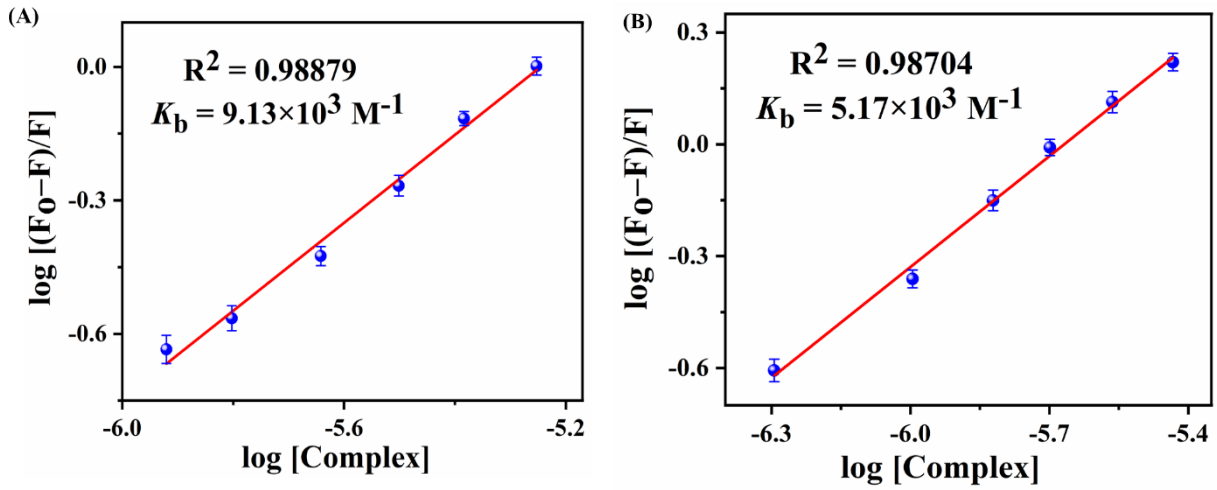

Fig. S30: Plot of log [(Fo-F)/F] versus log [Complex] for **HL^1** (A) and **HL^2** (B).

Table S9: Comparison table of IC_{50} values of similar palladium complexes.

Complex	**IC_{50} Values** (μM)	**Ref**
	MCF-7 cells	
C1	16.66	This work
C2	9.46	
[Pd(HL)(Cl)$_2$]	48.1	65
1	14.6	66
2	9.34	
3	7.56	
Pd1	11.2	50
Pd2	154.9	
Pd3	230.1	
Pd4	61.5	
2	26.49	51
3	36.42	

$$\text{Percentage (\%) Cell viability} = \frac{[(A_{treated} - A_{blank})]}{[(A_{untreated} - A_{blank})]} \times 100$$

Equation 1: The cell viability percentage formula